

The superconducting electronic heat capacities of V²² and Sn²³ have been shown to exhibit such an exponential temperature dependence for $t < 0.7$ with the values $a = 9.17$ and $b = 1.50$. The superconducting heat capacity of lanthanum goes nearly as T^3 at the lowest temperatures but with a negative intercept. In order to remain positive down to the absolute zero it must fall less rapidly, in a manner suggestive of Eq. (21). An attempt to fit the data of La III to the corresponding relation,

$$C_{es} = x\gamma_\alpha T_\alpha a e^{-bT_\alpha/T} + (1-x)\gamma_\beta T_\beta a e^{-bT_\beta/T}, \quad (22)$$

²² Corak, Goodman, Satterthwaite, and Wexler, Phys. Rev. **102**, 656 (1956).

²³ W. S. Corak and C. B. Satterthwaite, Phys. Rev. **102**, 662 (1956).

discloses small but systematic deviations. An approximate fit from 1.6 to 3.4°K, using the values $a = 9.20$ and $b = 1.58$, deviates by as much as 5% from the data.

IV. ACKNOWLEDGMENTS

It is a pleasure to acknowledge the cooperation of Professor F. H. Spedding and David Dennison of the Institute for Atomic Research at Ames, Iowa, in preparing the samples of lanthanum and supplying the analysis of impurities. We are indebted to the following for their assistance in making the measurements: Bruce J. Biavati, Alan T. Hirshfeld, Raymond Kaplan, Claire Metz, Dr. Bernard Smith, Professor Adam H. Spees, and Dr. R. D. Worley.

Double Electron Capture and Loss by Helium Ions Traversing Gases*

SAMUEL K. ALLISON

Enrico Fermi Institute for Nuclear Studies, University of Chicago, Chicago, Illinois

(Received August 28, 1957)

A beam of pure He⁺⁺ ions was passed through a cell in which the gas pressure could be varied, and the emergent beam was examined for its He⁰ and He⁺ content. With helium and air in the cell, it was observed that He⁰ persists to pressures so low that it could not have been formed except by double electron capture by He⁺⁺ in a single collision. In hydrogen the double capture event is much less probable.

The analogous experiment was performed with a helium atomic beam, and at 250 kev and 450 kev in air He⁺⁺, formed by double electron loss, was detected. In hydrogen and helium only upper limits for double electron loss could be established.

These results, with values of the sums $(\sigma_{20} + \sigma_{21})$ and $(\sigma_{01} + \sigma_{02})$ measured in previous researches, made it possible to compute values of σ_{20} and σ_{02} , as in the following table.

I. INTRODUCTION

THIS paper reports measurements of cross sections for charge-changing collisions of moving helium ions in gases. A kinetic energy range from 150 to 450 kev is covered, the corresponding velocities ranging between 1.22 and 2.12 times the Bohr electron velocity in the hydrogen atom, 2.18×10^8 cm/sec. In this region the charge-equilibrated helium beam must be considered at least a three-component system; the charge states He⁰, He⁺, He⁺⁺ all appear in the beam in fractions greater than 1%. For He⁰ the most probable charge-changing events are He⁰ → He⁺ and He⁰ → He⁺⁺, the cross sections for which are called σ_{01} and σ_{02} . For the other charge states the most probable charge changes on collision correspond to the cross sections σ_{10} , σ_{12} , σ_{20} , σ_{21} .

* This work was supported in part by the U. S. Atomic Energy Commission.

kev	Cross sections in units of 10^{-17} cm ² per atom					
	Hydrogen		Helium		Air	
	σ_{20}	σ_{20}/σ_{21}	σ_{20}	σ_{20}/σ_{21}	σ_{20}	σ_{20}/σ_{21}
<i>Double electron capture</i>						
150	1.1	0.04	5.7	0.30	11.8	0.24
250	0.87	0.06	2.7	0.19	5.2	0.15
350	0.20	0.03	1.1	0.10	2.1	0.09
450	0.12	0.05	1.1	0.15	1.3	0.08
<i>Double electron loss</i>						
	σ_{02}	σ_{02}/σ_{01}	σ_{02}	σ_{02}/σ_{01}	σ_{02}	σ_{02}/σ_{01}
250	0.1 ± 0.1	~0.02	0.2 ± 0.2	~0.02	0.5 ± 0.4	0.02
450	<0.1	<0.01	<0.2	<0.01	1.3 ± 0.4	0.06

A table of the six charge-changing collision cross sections for helium ions is presented. The equations needed to compute the change in the charge composition of a helium ion beam due to passage through a gas film are given.

The capture of two electrons by He⁺ in a single collision, leading to a negative helium ion, has been observed at kinetic energies as high as 160 kev, with σ_{11} ranging from 0.01×10^{-19} cm² in helium gas to 0.6×10^{-19} cm² in krypton,¹ but such events occur with a probability of the order of 0.10% of that of the others mentioned. No attempt was made in these experiments to observe negative helium ions.

Charge-changing cross-section measurements for helium beams have been described in two prior publications from this laboratory^{2,3} and the equipment used

¹ Dukel'skii, Afrosimov, and Fedorenko, Zhur. Eksptl. i Teort. Fiz. (U.S.S.R.) **30**, 792 (1956) [translation: Soviet Phys. JETP **3**, 764 (1956)]. The phenomenon of double electron capture had previously been observed in the case of protons, Ya. M. Fogel' and R. V. Mitlin, Zhur. Eksptl. i Teort. Fiz. (U.S.S.R.) **30**, 450 (1956) [translation: Soviet Phys. JETP **3**, 334 (1956)].

² S. Krasner, Phys. Rev. **99**, 520 (1955).

³ Allison, Cuevas, and Murphy, Phys. Rev. **102**, 1041 (1956); this will be referred to as ACM.

was similar to that of this earlier work. In our previous work the total attenuation of a single charge-component helium ion beam in a strong magnetic field was observed as minute amounts of gas were admitted. The attenuation takes place because any ion which changes its charge changes the radius of curvature of its path in the field and fails to enter the small aperture of a detector so placed as to collect the entire beam under high vacuum conditions. Such total attenuation experiments measure the sums

$$\alpha \equiv \sigma_{01} + \sigma_{02}, \quad \beta \equiv \sigma_{10} + \sigma_{12}, \quad \gamma \equiv \sigma_{20} + \sigma_{21}, \quad (1)$$

and do not in themselves give individual cross sections.

In order to compute the individual cross sections σ_{10} and σ_{12} , ACM made use of additional information, namely the equilibrated ratio $\text{He}^+/\text{He}^{++}$ as observed by Snitzer⁴ and by Stier, Barnett, and Evans⁵ in helium ion beams which have attained an invariant charge composition by traversing sufficiently thick gas films. Let $F_{0\infty}$, $F_{1\infty}$, $F_{2\infty}$ represent these equilibrated fractions; Allison and Warsaw⁶ have shown that

$$F_{1\infty}/F_{2\infty} = (\alpha\sigma_{21} + \sigma_{01}\sigma_{20})/(\beta\sigma_{02} + \sigma_{12}\sigma_{01}). \quad (2)$$

ACM assumed that σ_{02} could be neglected with respect to the other cross sections, so that

$$\sigma_{12} \doteq (\gamma F_{2\infty})/F_{1\infty}, \quad (3)$$

and thus they obtained values of σ_{12} , and of σ_{10} by subtraction from β . The extension of the experiments reported here shows that no serious errors in σ_{10} and σ_{12} were made by this neglect of σ_{02} ; if it has a value as high as the upper limit of approximately 0.3×10^{-17} cm² for H₂ and He gases at 150 kev, the ACM values of σ_{12} are reduced to about the lower limit of the range of uncertainty given by them (see Table V and ACM and Table VI of this paper).

ACM did not obtain separate values of σ_{20} and σ_{21} from their observed sum γ through an analogous use of the equilibrated ratio $F_{0\infty}/F_{2\infty}$. In the energy range of this work, the values of $F_{0\infty}$, $F_{1\infty}$, and $F_{2\infty}$ are quite insensitive to changes in ϵ , where

$$\epsilon \equiv \sigma_{20}/(\sigma_{20} + \sigma_{21}), \quad (4)$$

and auxiliary experiments must be performed to measure σ_{20} and σ_{21} as separated quantities. This paper describes such measurements, and analogous ones leading to the determination of

$$\epsilon' \equiv \sigma_{02}/(\sigma_{01} + \sigma_{02}). \quad (5)$$

II. MATHEMATICAL TREATMENT OF CHARGE EQUILIBRATION

The differential equations involved in describing changes in the charge composition of a three-component

system were stated in the review by Allison and Warsaw, and a solution appropriate to certain boundary conditions was presented.⁷ We need more general solutions for our present purpose, so the equations will be restated with slight improvements in notation. We deal with dimensionless quantities F_i which are the fractions of the total flux of ions which are in charge state $i|e|$, where $|e|$ is the magnitude of the electronic charge. Then the independent differential equations of interest are

$$dF_1/d\pi = F_0(\sigma_{01} - \sigma_{21}) - F_1(\sigma_{21} + \beta) + \sigma_{21}, \quad (6)$$

$$dF_0/d\pi = F_1(\sigma_{10} - \sigma_{20}) - F_0(\sigma_{20} + \alpha) + \sigma_{20}. \quad (7)$$

F_2 can always be found from

$$F_2 = 1 - (F_0 + F_1), \quad (8)$$

since we are neglecting the presence of negative helium ions. π represents the number of atoms of gas per cm² which the beam has traversed. If, as in the usual experimental situation, the beam passes from high vacuum into, and exits into high vacuum from, a compartment of length l cm which contains a gas having ξ atoms per molecule, at pressure p dynes/cm², then

$$\pi(p) = Ll\xi p/RT, \quad (9)$$

where L is Avogadro's number, R the gas constant (8.31×10^7 erg/mole °C), and T the absolute temperature.

It is convenient to introduce four new constants which are linear combinations of the cross sections:

$$\begin{aligned} a &\equiv -(\sigma_{21} + \beta), & f &\equiv \sigma_{10} - \sigma_{20}, \\ b &\equiv (\sigma_{01} - \sigma_{21}), & g &\equiv -(\sigma_{20} + \alpha), \end{aligned} \quad (10)$$

such that the differential Eqs. (6) and (7) become

$$\begin{aligned} dF_1/d\pi &= aF_1 + bF_0 + \sigma_{21}, \\ dF_0/d\pi &= fF_1 + gF_0 + \sigma_{20}. \end{aligned} \quad (11)$$

The solution of such equation sets is standard practice. The solutions may be summarized as follows:

$$F_i = F_{i\infty} + [P(z, i) \exp(\pi q) + N(z, i) \exp(-\pi q)] \exp(-\frac{1}{2}\pi \sum \sigma_{if}), \quad (12)$$

in which

$$q = +\frac{1}{2}[(g-a)^2 + 4bf]^{\frac{1}{2}}, \quad (13)$$

$$\sum \sigma_{if} = -(a+g), \quad (14)$$

$P(z, i)$ is a function of the cross sections applicable to the composition of the beam (index z) at $\pi=0$, and to the type of ion (i) whose participation in the beam is being discussed, and $N(z, i)$ is the analogous coefficient of the negative exponential.

Initial conditions of special interest are those in which the ions of the beam, traveling in high vacuum before entering the charge-changing compartment, are

⁴ E. Snitzer, Phys. Rev. **89**, 1237 (1953).

⁵ Stier, Barnett, and Evans, Phys. Rev. **96**, 973 (1954).

⁶ In the review article of S. K. Allison and S. D. Warsaw, Revs. Modern Phys. **25**, 779 (1953), these quantities are called ϕ_1 , ϕ_2 , ϕ_3 , and other authors have followed this notation.

⁷ Certain typographical errors in the solution were pointed out by J. A. Phillips and J. L. Tuck, Rev. Sci. Instr. **27**, 97 (1956).

TABLE I. Coefficients P and N for Eq. (12).

Original state ($\pi=0$)	$P(z,i)$	$N(z,i)$
A. To calculate changes in the fraction of He^+ present in a beam in which originally all the ions had the same charge.		
all He^0	$P(0,1) = \frac{1}{2q} [bF_{2\infty} + (b+s-q)F_{1\infty}]$	$N(0,1) = -\frac{1}{2q} [bF_{2\infty} + (b+s+q)F_{1\infty}]$
all He^+	$P(1,1) = -\frac{1}{2q} [(s-q)(1-F_{1\infty}) + bF_{0\infty}]$	$N(1,1) = -\frac{1}{2q} [(s+q)(1-F_{1\infty}) + bF_{0\infty}]$
all He^{++}	$P(2,1) = \frac{1}{2q} [F_{1\infty}(s-q) - bF_{0\infty}]$	$N(2,1) = -\frac{1}{2q} [F_{1\infty}(s+q) - bF_{0\infty}]$
B. To calculate changes in the fraction of He^0 present in a beam in which originally all the ions had the same charge.		
$z e $	$P(z,0) = P(z,1)(s+q)/b$ $z=0, 1, 2$	$N(z,0) = N(z,1)(s-q)/b$ $z=0, 1, 2$
C. To calculate changes in the fraction of He^{++} present in a beam in which originally all the ions had the same charge.		
$z e $	$P(z,2) = -P(z,1)(b+s+q)/b$ $z=0, 1, 2$	$N(z,2) = -N(z,1)(b+s-q)/b$ $z=0, 1, 2$

all of the same charge. Thus, $P(0,1)$ represents the appropriate coefficient for the growth of He^+ in a beam which was originally 100% He^0 .

In all cases of physical interest, $\frac{1}{2}\sum \sigma_{if} > q$, so that in the limit $\pi \rightarrow \infty$ the term in Eq. (12) involving exponentials becomes zero, leaving

$$F_{i\infty} = \lim_{\pi \rightarrow \infty} F_i. \quad (15)$$

In terms of the cross sections, the equilibrated fractions $F_{i\infty}$ are

$$F_{0\infty} = (f\sigma_{21} - a\sigma_{20})/D = (\beta\sigma_{20} + \sigma_{10}\sigma_{21})/D, \quad (16)$$

$$F_{1\infty} = (b\sigma_{20} - g\sigma_{21})/D = (\alpha\sigma_{21} + \sigma_{01}\sigma_{20})/D, \quad (17)$$

$$F_{2\infty} = [\sigma_{20}(a-b) + g(a+\sigma_{21}) - f(b+\sigma_{21})]/D, \quad (18)$$

where

$$D = ag - bf = \sigma_{12}(\alpha + \sigma_{20}) + \sigma_{10}(\gamma + \sigma_{02}) + \alpha\sigma_{21} + \sigma_{01}\sigma_{20}. \quad (19)$$

Table I gives the expressions for $P(z,i)$ and $N(z,i)$ appropriate to the different beam constituents and to the three unmixed initial states. In this table the symbol

$$s \equiv \frac{1}{2}(g-a) \quad (20)$$

appears. The following relations between the N 's, P 's, and F 's are useful in checking the internal consistency

$$\frac{F_0}{F_1} = \frac{F_{0\infty} + [P(2,0) \exp(\pi q) + N(2,0) \exp(-\pi q)] \exp(-\frac{1}{2}\pi \sum \sigma_{if})}{F_{1\infty} + [P(2,1) \exp(\pi q) + N(2,1) \exp(-\pi q)] \exp(-\frac{1}{2}\pi \sum \sigma_{if})}. \quad (24)$$

In passing to the limiting value at $\pi=0$, as a first step we expand the exponentials and retain only the first power of the exponents. Using Table IB to eliminate $P(2,0)$ and $N(2,0)$, and making use of Eq. (21), we

of a set of numerical values:

$$F_{i\infty} = -[P(z,i) + N(z,i)], \quad z \neq i; \quad (21)$$

$$1 - F_{i\infty} = [P(z,i) + N(z,i)], \quad z = i. \quad (22)$$

III. EXPERIMENTAL METHOD

Since the previous ACM measurements have given us, for instance, $\gamma = \sigma_{20} + \sigma_{21}$, experimental measurement of ϵ [Eq. (4)] would establish the individual values of σ_{20} and σ_{21} . The quantity ϵ may be measured by allowing a beam of He^{++} ions to pass through a gas cell, and lowering the gas pressure until one observes

$$\lim_{\pi \rightarrow 0} \left(\frac{F_0}{F_1} \right) = \frac{\sigma_{20}}{\sigma_{21}} = \frac{\epsilon}{1 - \epsilon} \quad (23)$$

in the emergent beam. Stated in other words, we create in the path of the He^{++} beam a "film" of gas so thin that the probability of two successive collisions of a moving helium ion with a target of atomic size is negligible. Then if He^0 appears in the emergent beam in appreciable ratio to He^+ , it must have been created in a single encounter in which He^{++} has captured two electrons.

The physically obvious result expressed in Eq. (23) may be formally deduced from Eq. (12) and provides an illustration of the use of Table I. Since we begin with a pure He^{++} beam ($z=2$), by Eq. (12) we have

obtain

$$\lim_{\pi \rightarrow 0} \left(\frac{F_0}{F_1} \right) = \frac{F_{0\infty}(\frac{1}{2}\sum \sigma_{if} - s) - fF_{1\infty}}{F_{1\infty}(\frac{1}{2}\sum \sigma_{if} + s) - bF_{0\infty}}. \quad (25)$$

The parenthetical expressions in the numerator and denominator may be reduced through Eqs. (14) and (20), and the result of Eq. (23) obtained using Eqs. (16) and (17).

The ratio $\lim_{\pi \rightarrow 0}(F_0/F_1)$ will be a sensitive test for the presence of double electron capture, since it will be zero if such events do not occur, and infinity if double capture were the only charge-changing collision experienced by He^{++} .

Actually the experimenter is faced by the necessity of a compromise; if he makes the gas film very thin to approach as nearly as possible the limit $\pi=0$, his accuracy will suffer because not enough He^0 and He^+ are produced for reliable detection. On the other hand, if he increases the film thickness to produce more He^0 and He^+ , the observed F_0/F_1 ratio becomes a less sensitive detector of the presence of double capture. As a preliminary to the experiments on double capture in air, a set of curves was calculated to indicate a good range of π . In estimating the initial stages of charge equilibration of a pure He^{++} beam, it can provisionally be assumed that ϵ' of Eq. (5) is zero; then the experiments of ACM provide us with σ_{01} , σ_{10} , σ_{12} , and γ . We assume various values of ϵ and calculate from Eq. (24), without approximating the exponentials, the expected behavior of the F_0/F_1 with changing π for each assumed ϵ . Such a family of curves is shown in Fig. 1.

For rapid physical interpretation of all the graphs in this paper, we have replaced π by the equivalent product (pl) , given [see Eq. (9)] by

$$(pl) = (\pi RT)/(L\xi). \quad (26)$$

We shall speak of the product (pl) as the "thickness" of the gas film, using p in microns of mercury and l in centimeters. The temperature is considered to be 293°K. Numerically, in these units, we have

$$\begin{aligned} \text{monatomic gas: } \pi &= 3.30 \times 10^{13} (pl), \\ \text{diatomic gas: } \pi &= 6.61 \times 10^{13} (pl). \end{aligned} \quad (26a)$$

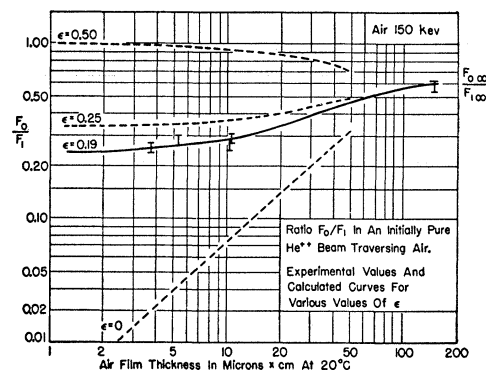


FIG. 1. Observed and calculated He^0/He^+ ratios produced in a He^{++} beam by charge-changing collisions in thin air films. The best fit requires a finite σ_{20} with $\epsilon = \sigma_{20}/(\sigma_{20} + \sigma_{21}) = 0.19$.

The curves of Fig. 1 were computed for a 150-keV helium beam in air. The cross sections used in the computation were, from ACM, $\sigma_{01} = 34.1$, $\sigma_{10} = 20.4$, $\sigma_{12} = 1.2$, and $\gamma = 62$ in units of 10^{-17} cm^2 . Curves were computed for $\epsilon = 0, 0.25, 0.50$, and later, as indicated by the experimental results, for $\epsilon = 0.19$. For $\epsilon = 0.19$, $P(2,0) = -1.104$, $N(2,0) = 0.738$, $P(2,1) = 0.979$, and $N(2,1) = -1.595$ in Eq. (24). The curves of Fig. 1 show clearly the enhanced sensitivity of the ratio to the presence of double electron capture at low (pl) values, and the relative insensitivity as equilibrium is approached.

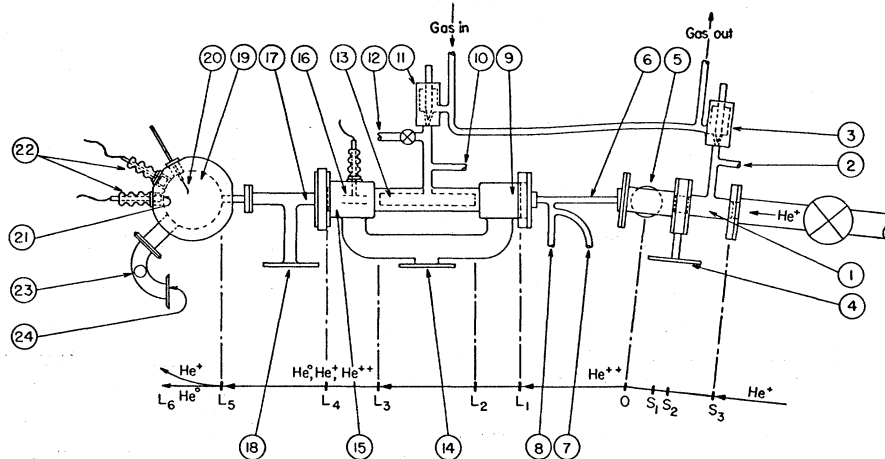
It is clear that double electron loss can be searched for in a similar manner, namely by preparing a beam of pure He^0 and finding experimentally

$$\lim_{\pi \rightarrow 0} \left(\frac{F_2}{F_1} \right) = \frac{\sigma_{02}}{\sigma_{01}} = \frac{\epsilon'}{1 - \epsilon'}. \quad (27)$$

IV. APPARATUS

Figure 2 shows a schematized drawing of the apparatus as it was used in the double-capture experiments.

FIG. 2. Schematized drawing of apparatus for producing and analyzing charge-changing collisions of He^{++} ions in gas films.



† See Table VI for better values of α and σ_{01} ; the result of this computation is, however, unaffected by such a change.

TABLE II. Description and dimensions of items shown in Fig. 2, as used in double electron capture experiments.

A. Description of items			
Item in Fig. 2	Description		
1	Equilibration cell for production of He^{++} from He^+ .		
2	To thermocouple vacuum gauge.		
3	Needle valve No. 1.		
4	To cold trap ^a and oil diffusion pump <i>A</i> .		
5	Magnet for selecting He^{++} . (Angle of deviation is $\tan^{-1}0.10$.)		
6	Beam traverse tube <i>A</i> .		
7	To cold trap and mercury diffusion pump <i>B</i> .		
8	To cold trap and McLeod gauge.		
9	Intermediate pressure compartment <i>A</i> .		
10	To cold trap and McLeod gauge.		
11	Needle valve No. 2.		
12	By-pass to cold trap and oil diffusion pump <i>C</i> .		
13	Charge changing cell.		
14	To cold trap and oil diffusion pump <i>C</i> .		
15	Intermediate pressure compartment <i>B</i> .		
16	Parallel-plate ionization chamber for beam monitoring.		
17	Beam traverse tube <i>B</i> (steel).		
18	To cold trap and oil diffusion pump <i>D</i> .		
19	Magnetic analysis chamber (see Krasner, ^b Fig. 4).		
20	Movable shutter for interrupting He^0 beam.		
21	Location of gold foils for equilibration before detection.		
22	Secondary electron emission beam detectors (see Montague ^c).		
23	To cold trap and McLeod gauge.		
24	To cold trap and oil diffusion pump <i>D</i> .		

B. Dimensions			
Item in Fig. 2	Traverse length in cm	Item in Fig. 2	Aperture diameter in cm
S_3S_2	10.8	S_3	0.159
S_2S_1	2.2	S_2	0.159
S_1O	4.7	S_1	0.150
OL_1	26.7	L_1	0.226
L_1L_2	8.3	L_2	0.091
L_2L_3	20.6	L_3	0.091
L_3L_4	8.3	L_4	0.226
L_4L_5	17.8		
L_5L_6	12.7		

^a All cold traps were cooled with liquid nitrogen.

^b See reference 2.

^c J. H. Montague, Phys. Rev. **81**, 1026 (1951), Fig. 2.

A Cockcroft-Walton accelerator (kevatron) provided a He^+ beam in the kinetic energy range 150 to 450 keV, and had associated with it a beam sorting magnet which deviated the He^+ 22.5° into the measuring equipment. Table II describes the various parts and gives significant linear dimensions and aperture diameters.

A He^{++} beam for double-capture measurements was produced in the equilibration compartment (1) where a gas film with (ρl) between 50 and 100 was created, using the same gas as was being admitted through needle valve No. 2 to the charge-changing cell (13). The limiting apertures on the He^{++} beam, selected from the mixed, equilibrated beam by the second sorting magnet (5) were at the entrance and exit of the charge-changing cell (L_2 and L_3).

In the double electron capture experiment it was necessary to compare the intensities of two differently charged beams (He^0 and He^+) as measured in different

secondary-electron detectors. The question arises as to whether the number of secondary electrons per incident ion is the same if the kinetic energies are equal but the ionic charges are not. This problem, the solution of which is part, but not all, of the detector calibration, was removed by equilibrating each beam in a thin gold foil (0.19 mg/cm^2) just before it enters the detector. Thus, the detector sees the same ionic mixture irrespective of the original beam composition, since the beams being compared have the same velocity. Other aspects of the detector problem are considered in the following section.

The currents from the detectors, which were biased -45 volts to saturate the secondary electron current,⁸ were of the order of 10^{-10} ampere, and the currents from the ionization chamber (16) were 10^{-11} ampere except in experiments on the He^{++} beam produced from 150-keV He^+ ions, where currents were lower by a factor 10.

To minimize the effect of the changes in the stray magnetic field on the secondary electron current from the detector, the design was such that from every point on the electron emitting surface which could be struck by the helium beam, the secondaries could complete the electrical circuit by a short vacuum path (0.5–0.8 cm) parallel to the lines of force of the magnetic field.

The detector currents fluctuated not only because of the intensity fluctuations in the kevatron beam but also because, due to the very high angular selectivity of the small apertures through which the beam was magnetically directed, the slightest energy fluctuation in the kevatron varied the intensity at the detector and monitor. Thus, it was necessary to integrate both monitor and detector currents with respect to time for reliable readings. A Brown electrometer and a vibrating-reed electrometer with multiple scale recorders were used on the monitor and detector, respectively. The instruments read the rate of rise of voltage on high quality capacitors into which the currents flowed. A specially constructed switch shifted the vibrating-reed electrometer from one detector to the other.

In the experiments on double electron loss, traverse tube *A* (Fig. 2, item 6) was replaced by a straight tube, so that the entire system from S_3 to L_5 was in the same straight line. The magnet at (5) was used to discard the He^{++} and He^+ constituents from cell (1), allowing the pure He^0 beam to pass through the aperture at L_1 .

Other parts of the apparatus, not specifically mentioned here, were as described in previous publications.^{2,3}

V. TESTS FOR SYSTEMATIC ERRORS, AND EXPERIMENTAL PROCEDURES

The history of attempts to measure electron capture and loss cross sections shows that in this field systematic errors are very likely to occur. There is no theory

⁸ Of course the charged ions in the equilibrated beams contributed to the detector current, but detector bias curves showed that more than 90% of the current was caused by secondaries.

reliable enough to enable the rejection of experimental results as being too improbable. Therefore many tests of the internal consistency of the measurements were made.

A. Detector Sensitivity

In the double-capture experiments it was necessary to calibrate the two detectors as to their secondary-electron-emitting efficiencies. The F_2/F_1 determination for double loss was simpler; here both beams could be magnetically deviated and thus alternately measured in the same detector. It was however, necessary to investigate whether the detector used was sensitive to the necessary magnetic field changes.

The two detectors were geometrically identical and were distinguished by spots of orange and black paint respectively. They were constructed at different times, however, and it is not certain that the same sheet of beryllium copper was used for the secondary-emitting surface.

Test 1. Interchange of detectors.—In one such test, a 250-keV He^{++} beam was passed through an airfilm with $pl \sim 3$ micron cm and the total (magnetic field zero) mixed beam measured in the orange detector at the 0° port. Then the magnet (at 19, Fig. 2) was switched on and the He^{++} constituent directed to the black detector at the 30° port. The apparent value of F_2 was 0.47. The beam valve to the kevatron was then shut and the detecting system filled with helium. The detectors were pulled out of their sockets and interchanged, with perhaps 15 seconds exposure to the air. In ten minutes the vacuum was re-established and readings could be taken again; now the apparent value of F_2 was 2.27. It is only necessary to assume that the effect of the magnetic field, if any, on the detector response was the same for both to deduce that the orange detector was the better secondary electron emitter by a factor $(2.27/0.47)^{1/2} = 2.2$, and that the true value of F_2 was essentially one, within 10%.

This calibration did not demonstrate that the detectors were unaffected by the magnetic field, and is open to the criticism that the secondary-electron-emitting surfaces might be altered in their brief exposure to air.

Test 2. Separation and reassembly of beam constituents.—As an illustration of this type of test, we describe one carried out under the same beam conditions as just previously mentioned in the example of Test 1. With the orange detector at the 0° port, the integrated response for a given monitor integration was proportional to 100, with no magnetic field on (at 19, Fig. 2) and the entire mixed beam entering. The magnetic field was then established and varied so that first the He^{++} and then the He^+ constituent was directed to the black detector at the 30° aperture; the integrated responses were 47 and 5 units respectively. The He^0 beam, left in the orange detector, gave 1.3 units; for simplicity this was divided by the factor 2.2 obtained

in Test 1, and added to the sum of He^{++} and He^+ in the black detector, making the total black detector response to the three parts of the beam 52.6 units. Comparison with the response of the orange detector to the total beam indicates that it is the more sensitive by a factor 1.9, in reasonable agreement with Test 1, and showing that the effect of the magnetic field on the detector response is less than 15%.

Every beam-ratio experiment where both detectors were involved was immediately preceded by a detector sensitivity test of type 2. Interchange of detectors, as in Test 1, was occasionally used. The factor in favor of the orange detector varied from 1.5 to 2.1 over the kinetic energy range of the experiments and the 10-week interval during which the final readings were taken.

For the F_2/F_1 measurements for the double electron loss, both the He^{++} and He^+ beams were alternately measured in the black detector at the 30° port. The beam shutter shown in Fig. 2 was removed and the orange detector placed in the 60° port, and occasionally the He^{++} beam was measured there. Applying the known sensitivity factor gave F_2/F_1 ratios agreeing with the single detector measurement.

B. (pl) Measurements

Although most of the charge-changing collisions took place in cell 13 of Fig. 1, collisions affecting the result were possible in the entire length OL_5 , a distance of 81.7 cm. The total film thickness was computed from the individual (pl) values indicated by McCleod gauge readings at the three locations shown in Fig. 2, plus an estimate of the (pl) in compartments (9) and (15). The latter estimate could be made as a result of previous experience with this equipment; and was a small correction.

C. Lowest (pl) Attainable

The method of taking data and their interpretation was much affected by the fact that even with both needle valves shut there was enough residual gas ($pl \sim 3$ micron cm) to cause more than 1% of He^+ to appear from a pure He^{++} or He^0 beam selected at (5), Fig. 2. If it was necessary to open needle valve No. 1 to obtain more He^{++} or He^0 , the pressure rose in the region OL_1 , and a higher fraction of the pure beam was converted prior to the intentional interposition of the gas film by opening needle valve No. 2.

The interpretation of measurements in air was less complicated than in other gases, since it could be assumed that the residual gas was air itself. The behavior of the F_0/F_1 ratio from a pure He^{++} beam as air film thickness is reduced is shown in the experimental points of Fig. 1. The result must be defended against the following criticism. Is the persistence of He^0 at the low (pl) values merely the result of equilibration of part of the He^{++} beam by scattering from metal aperture edges in its long path? In refutation it

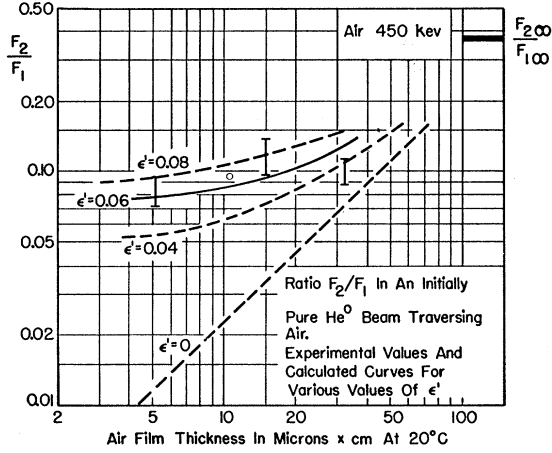


FIG. 3. Observed and calculated $\text{He}^{++}/\text{He}^+$ ratios produced in the He^0 beam by charge-changing collisions in thin air films. The best fit requires a finite σ_{02} , with $\epsilon' = \sigma_{02}/(\sigma_{02} + \sigma_{01}) = 0.06$.

can be calculated that the amounts of ($\text{He}^0 + \text{He}^+$) observed at the lowest (pl) values can be accounted for as having been produced in the gas film. As an example, consider the experimental value of $F_0/F_1 = 0.28$ at (pl) = 5.4 in Fig. 1. Here the measured intensities were $\text{He}^0 = 0.34$, $\text{He}^+ = 1.22$, $\text{He}^{++} = 6.12$ so that $(F_0 + F_1) = 1.56/7.6 = 0.20$. From Eqs. (26a), $\pi = 3.57 \times 10^{14}$, and using the P and N values given in the discussion of Fig. 1 we can compute F_0 and F_1 from Eq. (12). We find $(F_0 + F_1) = 0.21 \pm 0.02$, which accounts for the observation, and similar agreement was obtained for the low (pl) points in other cases.

Further evidence lies in the fact that as the gas film thickness was increased (see Fig. 1), the ratio F_0/F_1 changed only slowly although there could be no doubt that the gas was increasing the intensities of both the He^0 and He^+ constituents. One would not expect an F_0/F_1 ratio contributed by aperture edge effects to be the same as that produced in the thin gas films.

$$\frac{F_2}{F_1} = \frac{F_{2\infty} + [P(0,2) \exp(\pi q) + N(0,2) \exp(-\pi q)] \exp(-\frac{1}{2}\pi \sum \sigma_{if})}{F_{1\infty} + [P(0,1) \exp(\pi q) + N(0,1) \exp(-\pi q)] \exp(-\frac{1}{2}\pi \sum \sigma_{if})} \quad (28)$$

Figure 3 shows such a family of curves for 450-keV helium ions in air, using $\alpha = 43.9$,[†] $\sigma_{10} = 4.0$, $\sigma_{12} = 6.6$, $\sigma_{20} = 1.3$, $\sigma_{21} = 16.9$ in units of 10^{-17} cm^2 and values of σ_{02} obtained for $\epsilon' = 0, 0.04, 0.06$, and 0.08 in $\sigma_{02} = \epsilon' \alpha$. As anticipated by ACM, the cross sections σ_{02} are relatively small. The accuracy is poor in Fig. 3 largely

TABLE III. Experimentally determined values of $\epsilon = \sigma_{20}/(\sigma_{20} + \sigma_{21})$, $\epsilon' = \sigma_{02}/(\sigma_{01} + \sigma_{02})$ for helium ions in air.

Kinetic energy (keV)	ϵ	ϵ'
150	0.190 ± 0.02	...
250	0.130 ± 0.02	0.02 ± 0.02
350	0.079 ± 0.006	...
450	0.072 ± 0.006	0.06 ± 0.02

D. Backgrounds

The background under the He^+ or He^{++} peaks could always be obtained by shifting the beam out of the detector aperture by a small change in the magnetic field at 19, Fig. 2. The background under He^0 was obtained by cutting off the beam with the shutter (20) which was so arranged that it did not intercept the other beams.

E. Gases

Measurements were taken in hydrogen, helium, and air. Oxygen in the electrolytic hydrogen was combined by a catalyst and the water frozen out. Government grade A helium was used. No purification was attempted for air. All calculations were made for 20°C . The gases continually flowed past the needle valves, at slightly above atmospheric pressure.

VI. INTERPRETATION OF MEASUREMENTS AND RESULTS

A. Air

Double electron capture experiments in thin air films were interpreted as indicated in Fig. 1. Curves showing F_0/F_1 against (pl) were calculated as indicated in Sec. III for various assumed values of ϵ , and the best fit to the experimental points decided the value of this ratio. Data were taken at 150, 250, 350, and 450 keV with results as shown in Table III.

Investigations of the probability of double electron loss from He^0 were carried out at 250 and 450 keV. These investigations followed the double electron capture experiments, so that σ_{20} and σ_{21} were separately known in addition to the cross sections given by ACM. Calculations of expected values of F_2/F_1 were carried out using

because only 7% of the original He^+ beam can be converted to He^0 in the first place. The evidence is, however, that $\epsilon' = 0.06 \pm 0.02$; see Table III.

B. Hydrogen and Helium

Deduction of values of ϵ and ϵ' from data in these light gases was carried out in a manner different from that described for air. This was necessitated by the fact, mentioned previously, that there was always a residual air film producing its contribution to the conversion of the He^{++} or the He^0 beam.

The procedure will be illustrated by giving as an example the interpretation of the data on double electron capture in helium gas by a 250-keV He^{++} beam.

The following measurements were made:

	Run 1	Run 2
π_a , the number of atoms of air per cm^2 in the residual gas film.	1.48×10^{14}	1.48×10^{14}
π_h , number of helium atoms per cm^2 added to the air film	5.03×10^{14}	10.99×10^{14}
$(F_0/F_1)_T$ observed from the helium-air mixture	0.196 ± 0.015	0.214 ± 0.015

For the interpretation a table of $\bar{\sigma}_{if}$ values per average atom in the gas mixture was computed, using

$$\bar{\sigma} = (\pi_a \sigma_a + \pi_h \sigma_h) / (\pi_a + \pi_h).$$

Using the ACM cross sections and assuming σ_{02} in helium to be zero, we obtain

	Run 1	Run 2
$\bar{\sigma}_{01}$ ($10^{-17} \text{ cm}^2/\text{atom}$)	19.0	16.4
$\bar{\sigma}_{02}^2$	0.17	0.09
$\bar{\sigma}_{10}$	7.5	6.9
$\bar{\sigma}_{12}$	1.45	1.24
$\bar{\gamma}$	21.9	19.4

If we now assume various values of ϵ for helium, we can calculate values of $(F_0/F_1)_T$ to be expected from the two gas mixtures, using Eq. (24). The result appears in Fig. 4. The dashed curves are computed curves for the two mixtures, and the solid intervals in them show where they pass through the regions of the experimental observations. The projections of these arcs on the ϵ axis give the value for pure helium, and the result is 0.165 ± 0.015 . The correction for residual air is in this case negligible; if the mixture had been treated as pure helium the result for ϵ would have been 0.170. In certain hydrogen-air mixtures, however, the correction was not small.

An exactly analogous procedure was used to find ϵ' for hydrogen and helium from $(F_2/F_1)_T$ measurements.

TABLE IV. Results on double electron capture in hydrogen and helium. $\epsilon = \sigma_{20}/(\sigma_{20} + \sigma_{21})$.

He ⁺⁺ Ion kinetic energy (kev)	Gas	Atoms air per $\text{cm}^2 \times 10^{14}$	Atoms gas per $\text{cm}^2 \times 10^{14}$	$(F_0/F_1)_T$	ϵ	ϵ adopted
150	H ₂	1.34	5.44	0.14 ± 0.01	0.04	0.04 ± 0.02
		1.93	12.41	0.16 ± 0.02	0.05	
	He	1.35	2.63	0.31 ± 0.03	0.22	0.23 ± 0.02
		1.35	4.57	0.36 ± 0.04	0.24	
250	H ₂	1.48	11.05	0.10 ± 0.01	0.054	0.06 ± 0.01
		1.48	19.96	0.12 ± 0.01	0.068	
	He	1.48	5.03	0.20 ± 0.02	0.17	0.16 ± 0.02
		1.48	11.00	0.20 ± 0.02	0.16	
350	H ₂	1.82	12.08	0.059 ± 0.006	0.027	0.028 ± 0.003
		1.82	21.46	0.060 ± 0.006	0.031	
	He	2.03	4.78	0.098 ± 0.01	0.077	0.090 ± 0.01
		2.03	9.56	0.12 ± 0.01	0.10	
450	H ₂	1.06	30.15	0.049 ± 0.005	0.041	0.050 ± 0.01
		1.06	52.49	0.061 ± 0.006	0.059	
	He	2.03	12.90	0.12 ± 0.01	0.11	0.13 ± 0.02
		2.03	29.13	0.15 ± 0.02	0.16	

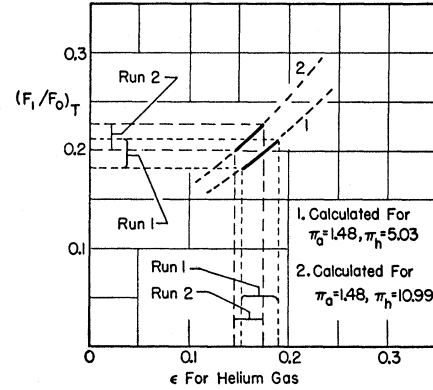


FIG. 4. $(F_0/F_1)_T$ is the ratio He^0/He^+ observed in a He^{++} beam undergoing charge-changing collisions in helium gas with air impurity. Corresponding values of $\epsilon = \sigma_{20}/(\sigma_{20} + \sigma_{21})$ in pure helium lie on the axis of abscissas.

Results for ϵ and ϵ' in hydrogen and helium are given in Tables IV and V. A collected table of the six σ 's for helium, based on ACM,³ Stier, Barnett, and Evans,⁵ and work in this laboratory is given as Table VI.

VII. DISCUSSION

The fraction σ_{20}/σ_{21} , the probability for double electron capture relative to that for a single capture collision, is shown in Fig. 5. We note at once the relative improbability of double electron capture in hydrogen. At 150 keV the probability of both electrons transferring from a helium atom to a He^{++} ion is 5.7/19 or 0.3 that of single transfer. For the hydrogen molecule, although the double capture event would be exothermic to the extent of 28 electron volts, the ratio is only 2.2/52.8 or 0.04. It is not clear, however, that the big difference in behavior is due to a resonance interchange of electrons between He^0 and He^{++} , because in air the double to single capture ratio is also high, about 0.19 at this 150-keV energy. The difference between H_2 and air is probably due to the greater electron density in oxygen and nitrogen atoms in the target area. In helium, both the electron density and resonant effects may contribute.

TABLE V. Results on double electron loss in hydrogen and helium. $\epsilon' = \sigma_{02}/(\sigma_{01} + \sigma_{02})$.

Helium ion kinetic energy (kev)	Gas	Atoms air per $\text{cm}^2 \times 10^{14}$	Atoms gas per $\text{cm}^2 \times 10^{14}$	$(F_2/F_1)_T$	ϵ'	ϵ' adopted
250	H ₂	3.23	24.2	0.022	...	0.02 ± 0.02
		3.23	41.7	0.024	...	
	He	3.36	6.96	0.038	0.047 ± 0.02	0.02 ± 0.02
		3.36	14.31	0.030	0.020 ± 0.02	
450	H ₂	4.85	52.1	0.052	< 0.01	< 0.01
		4.85	101.3	0.057	< 0.01	
	He	5.91	24.1	0.070	< 0.01	< 0.01
		5.91	42.5	0.069	< 0.01	

TABLE VI. Charge-changing collision cross sections for helium ions in units of 10^{-17} cm² per atom of gas.

Kinetic energy (keV)	σ_{01}^b	σ_{02}^b	σ_{10}	σ_{12}	σ_{20}	σ_{21}
Hydrogen						
150	5.8 ± 0.3	...	6.8 ± 0.7	0.24 ± 0.04	1.1 ± 0.5	26.4 ± 3
250	5.7 ± 0.3	0.1 ± 0.1	$3.2, +0.2, -0.7$	0.64 ± 0.04	0.87 ± 0.3	$13.6, +2, -1$
350	6.0 ± 0.3	$< 0.1^a$	1.2 ± 0.2	0.98 ± 0.10	0.20 ± 0.18	6.8 ± 0.7
450	7.0 ± 0.4	< 0.1	0.70 ± 0.3	0.80 ± 0.08	0.12 ± 0.05	2.4 ± 0.3
Helium						
150	8.9 ± 0.4	...	$12.4, +3, -1$	0.64 ± 0.10	5.7 ± 0.6	19 ± 4
250	9.7 ± 0.5	0.2 ± 0.2	6.2 ± 0.7	$1.0, +0.2, -0.07$	2.7 ± 0.3	$14, +2, -1$
350	8.4 ± 0.4	$< 0.2^a$	3.1 ± 0.5	1.5 ± 0.1	1.1 ± 0.2	10.6 ± 1.2
450	8.2 ± 0.4	< 0.2	$1.5, +0.3, -0.7$	$1.9, +0.4, -0.03$	1.1 ± 0.2	$7.5, +1.5, -0.1$
Air						
150	21.0 ± 1	0.2 ± 0.2^a	20 ± 2.2	1.2 ± 0.2	11.8 ± 1.0	50 ± 5
250	22.7 ± 1	0.5 ± 0.4	12 ± 1.5	3.1 ± 0.2	5.2 ± 0.6	$35, +0, -2.5$
350	21.2 ± 1	0.8 ± 0.5^a	7.3 ± 1.3	5.1 ± 0.4	2.1 ± 0.2	$25, +0, -3$
450	23.2 ± 1	1.3 ± 0.4	4.0 ± 1.0	6.6 ± 0.4	1.3 ± 0.1	17 ± 1.5

^a Estimated by interpolation or extrapolation of measured values.

^b Based on recent, unpublished determinations of $(\sigma_{01} + \sigma_{02})$ which are more reliable than those in reference 2.

Figure 5 gives some evidence of a shallow minimum in the σ_{20}/σ_{21} ratio in helium at about 350 keV. Too much reliance should not be placed on this behavior since the evidence for it depends only on one experimental point.

Recently Gerasimenko and Rosentsveig⁹ have computed the double electron capture probability for fast He^{++} ions in helium gas. Their method of computation is one which lacks accuracy at the relatively low kinetic

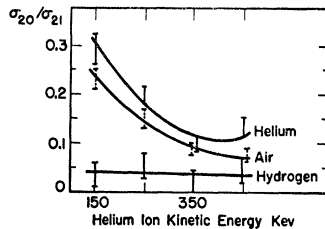


FIG. 5. Relative probability of double to single electron capture as a function of He^{++} -ion kinetic energy.

⁹ V. I. Gerasimenko and L. N. Rosentsveig, Zhur. Eksptl. i Teort. Fiz. (U.S.S.R.) **31**, 684 (1956) [translation: Soviet Phys. JETP **4**, 509 (1957)].

energies measured here, but indicates a rapid decrease in σ_{20} as the velocity increases, with a value about 6×10^{-17} cm² (twice that observed) at 250 keV.

Double electron loss by negative ions moving through gases has been observed by Dukel'skii and Fedorenko.¹⁰ In the present experiments, positive evidence for such a loss from helium atoms in motion is confined to 450-keV He^0 ions in air, and with a larger experimental error, 250-keV He^0 ions in air. Only upper limits could be assigned to σ_{02} in hydrogen and helium. In air the ratio σ_{02}/σ_{01} increases roughly by a factor of 3 between 250 and 450 keV, but σ_{01} itself is relatively constant. The fact that the double loss can be detected in air but not in H_2 or He is undoubtedly due to the more intense electric fields in the inner regions of oxygen and nitrogen atoms.

My thanks are due Mr. John Erwood for maintaining the equipment and assisting in taking readings.

¹⁰ V. M. Dukel'skii and N. V. Fedorenko, Zhur. Eksptl. i Teort. Fiz. (U.S.S.R.) **29**, 473 (1955) [translation: Soviet Phys. JETP **2**, 307 (1956)].